Vol. 493: 9–21, 2013
doi: 10.3354/meps10514

MARINE ECOLOGY PROGRESS SERIES
Mar Ecol Prog Ser

Published November 20

FREE ACCESS

N_2 fluxes in sediments of the Elbe Estuary and adjacent coastal zones

Astrid Deek[1,2,*], Kirstin Dähnke[1,*,], Justus van Beusekom[1], Sven Meyer[3], Maren Voss[3], Kay Emeis[1,2]**

[1]Helmholtz Zentrum Geesthacht, Institute of Coastal Research, 21502 Geesthacht, Germany
[2]IfBM, University of Hamburg, 20146 Hamburg, Germany
[3]Baltic Sea Research Institute, 18119 Rostock, Germany

ABSTRACT: The conversion of reactive nitrogen species to N_2 during denitrification in sediments may be one of the most valuable ecosystem services provided by estuarine and intertidal environments near river discharge areas. To quantify the rates and limiting factors of denitrification in the estuary of the Elbe River and adjacent Wadden Sea (SE North Sea), we measured sediment N_2 fluxes across subtidal and intertidal sediments, and along gradients in nitrate and organic matter concentrations. We conducted 2 sampling campaigns, in March and September 2009, during which N_2 fluxes were quantified by N_2/Ar measurements in sediment core incubations, and compared to isotope pairing results in September 2009. At ambient nitrate concentrations, sediments in the inner Elbe Estuary produced N_2 fluxes of up to 156 µmol N m^{-2} h^{-1}. In September, nitrate concentration in bottom water and organic matter content in sediments limited N_2 production; such limitations were not observed in March. We extrapolated the estuarine sediment nitrogen removal of March and September to the present-day area of intertidal and subtidal sediments in the Elbe Estuary between the port of Hamburg and the transition to the North Sea. Our estimate suggests that 3.3 ± 1.2 kt nitrate-N are removed in sediments in this region in spring and summer. This implies that reactive nitrogen removal in the inner Elbe Estuary reduces the spring/summer load of the Elbe River (47 kt N) by around 7%, a reduction that is much lower than commonly assumed for estuaries, and significantly lower than nitrate removal in the Elbe was in historical times.

KEY WORDS: Denitrification · Nitrogen cycle · Eutrophication · Elbe Estuary

INTRODUCTION

Anthropogenic nitrogen burdens on the global environment have increased during the last century (Erisman & Sutton 2008) but are an inevitable consequence of growing populations and food production, and increasingly of biofuel production. Because excessive discharge of reactive (bio-available) nitrogen (N_r) by rivers and atmospheric fluxes into the coastal ocean is known to compromise its ecosystem structure and functions, significant efforts have been invested and are being demanded by legislation to reduce river loads in Europe and elsewhere.

Estuaries, the mixing zones of river water and marine waters, attenuate land-sea fluxes of N_r. Although variable tidal amplitudes and riverine inputs create significant differences among individual estuaries (Day et al. 1989), they are all hotspots of biogeochemical cycling (Conley et al. 2000), where river loads of nutrients are rapidly turned over and in part removed before export to coastal waters. This removal may be due both to anaerobic ammonium oxidation (anammox) and denitrification. Both processes convert bio-available nitrogen species to gaseous N_2, which then escapes to the overlying water and atmosphere (Nixon et al. 1996). Anammox and denitrification are of potential

*These authors contributed equally
**Corresponding author. Email: kirstin.daehnke@hzg.de

importance in estuarine sediments, and act as significant sinks for N_r and first order regulation mechanisms for eutrophication in coastal seas (Seitzinger 1988, Middelburg et al. 1996). Generally, it is assumed that denitrification is quantitatively more important than anammox in shallow, organic-rich sediments (Thamdrup & Dalsgaard 2002, Thamdrup 2012).

Over the last 40 yr, the industrialization of rivers and estuaries discharging into the North Sea has created environments that are less effective filters of land-sea matter fluxes. The Elbe River is an example of such a highly managed river system: flood protection has significantly reduced intertidal areas and wetlands, and the riverbed of the Elbe River has been continuously dredged to maintain the water route to Germany's largest port in Hamburg (Lozán & Kausch 1996, Heise et al. 2005). While Schröder et al. (1996) estimated a sedimentary N_r removal of about 40% of the upstream riverine load in the 1980s, recent nitrate isotope studies suggest that the Elbe Estuary of the 2000s has become a mere conduit for river-borne nitrate loads, and shows no sign of significant N_r removal (Dähnke et al. 2008).

While the overall trend of riverine N-loads shows a gradual decrease over time (Pätsch & Lenhart 2011), this trend may be reversed in light of the expected increase in river-borne loads of N_r due to increased biofuel production in the catchment. Furthermore, riverine N loads can be modified in the estuary, where nitrate can either be removed via denitrification or produced by remineralisation and nitrification of sediment organic matter. This estuarine processing impacts the N loads that ultimately reach the coastal ocean. We therefore wished to re-evaluate the estuarine capacity for N_r removal in shallow water zones of the Elbe Estuary, and in subtidal and intertidal seafloors along the flow path of the Elbe River plume along the North Frisian Wadden Sea coast (Fig. 1). Previous work (Deek et al. 2011) showed that natural denitrification rates depend crucially on ambient nitrate concentrations at the sediment-water interface (as a function of season and distance from the river mouth), and on organic matter concentrations in sediments. Therefore, we selected different sediment types along the nitrate concentration gradient and analysed the flux of N_2 out of the sediments during 2 seasons.

Our main objective in this study was to quantify net N_2 production in the present-day Elbe Estuary, and to evaluate changes in nitrogen removal rates since historical times. Based on these data, we wanted to investigate whether the outlined changes are due to an altered sediment structure or function.

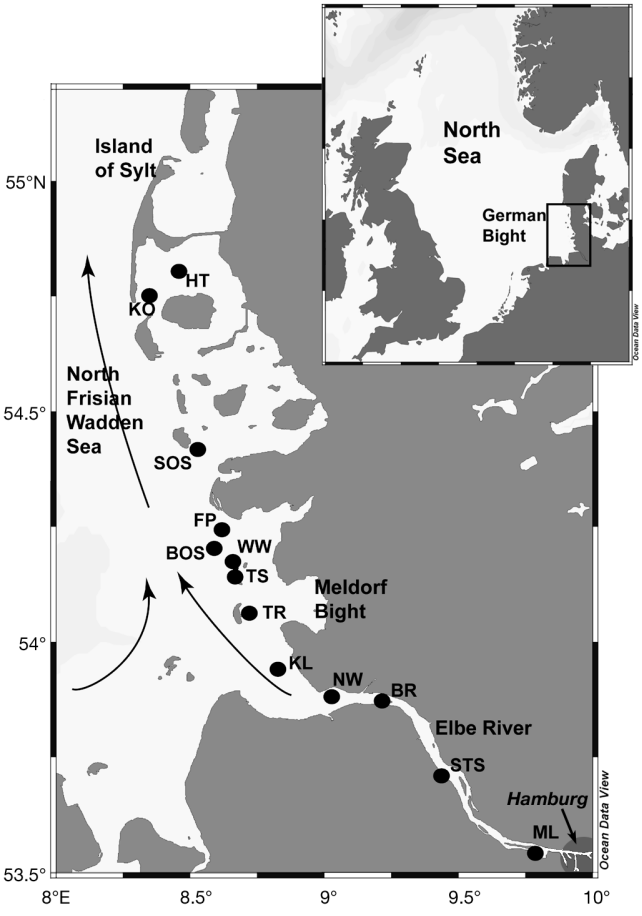

Fig. 1. Study sites. Arrows indicate general counter-clockwise water circulation in the study area

MATERIALS AND METHODS

Study site

The Elbe River is one of the main water routes of central Europe, and connects the port of Hamburg with a highly industrialized and farmed catchment area (Lozán & Kausch 1996). Between 2000 and 2010, the river had an average fresh water discharge of 731 $m^3 s^{-1}$ and delivered an average annual dissolved N_r load of 82 ± 24 kt (of which 3.9 ± 0.9 was ammonium) (Pätsch & Lenhart 2011) into the Elbe Estuary and SE North Sea. The nitrate discharge of the Elbe River is higher in winter than in summer. Consequently, in summer, elevated nitrate concentrations in coastal waters of low salinity are confined to south of the Meldorf Bight (Fig. 1), whereas the nitrate trace of the Elbe River plume extends to the northern Wadden Sea (as far as the island of Sylt; Fig. 1) in winter months (Brockmann & Kattner 1997, van Beusekom et al. 2008).

Sampling

Sediment samples were collected during 2 research cruises aboard the RV 'Ludwig Prandtl' in March and September 2009. During the campaign in March 2009, we sampled 7 stations, 5 in the inner estuary (Stns ML to KL), and 2 stations (Stns TS, WW) within the flow path of the river plume offshore (Table 1, Fig. 1). In September 2009, we sampled an extended set of 12 stations (Stns ML to HT; Fig. 1). At all stations, water temperature, salinity and O_2 saturation were measured with a multiprobe (OTS 1500, ME Meerestechnik-Elektronik). For continuous flow incubations, bottom water (min. 100 l each) and sediment cores of ~20 cm length and 10 cm diameter were taken with a multicorer (MUC). After sampling, we adjusted the water level overlying the sediment in the tubes to 10 cm. A subsample of filtered (0.2 µM PVDF) bottom water was stored at −20°C for nutrient analysis. During the sampling campaign in September 2009, we sampled additional sub-cores (25 cm length, 3.6 cm diameter) with a defined supernatant water column at 7 stations (Stns ML, BR, KL, TR, BOS, SOS, HT; Fig. 1) for subsequent isotope pairing, as described below. All sediment cores were cooled and transported within 6 h to the temperature-controlled laboratory.

Sediment core incubations

Denitrification can be measured by different techniques, the most common of which include determination of the N_2/Ar ratio (Kana et al. 1994) and the isotope pairing technique (IPT; Nielsen 1992, Steingruber et al. 2001). In our experiments, we incubated intact cores both with and without ^{15}N-tracer addition for N_2/Ar measurements. Furthermore, to compare the results of N_2/Ar measurements and IPT, we additionally used IPT in a subset of cores.

Continuous flow incubations with intact sediment cores. Before starting the sediment core incubations, the overlying water was aerated with aquarium pumps for 6 to 12 h to achieve 100% oxygen saturation. The incubation flow-through setup is a modified and larger version of the incubation procedure described in Gardner et al. (1991), Lavrentyev et al. (2000) and McCarthy & Gardner (2003), and is described in detail in Deek et al. (2011). Briefly, cores were incubated at *in situ* temperature in the dark, with an overlying water volume of 785 ml, continuously replaced by aerated site water at a rate of 1 to 2 ml min^{-1}.

Every 12 h of incubation, triplicate samples of inflow water and outflow water were analysed for N_2 and O_2 using a membrane inlet mass spectrometer (MIMS) as described below. To assess the contribution of water column denitrification, 2 control cores containing only site water were incubated correspondingly (Nielsen et al. 2000). Every 24 h, nutrient samples of inflow and outflow water were taken, filtered (0.2 µM PVDF) and stored frozen (−20°C) for later analysis. Nutrient and N_2 fluxes are reported only for the steady-state phase of the incubations, when fluxes had reached a plateau (between Days 2 and 6 of the incubations).

Flow-through incubations were done in 3 to 6 parallel sediment cores from each site. We performed 2 experiments: in one setup, rates were measured at ambient nitrate concentrations, and N_2 concentrations in the overlying water were calculated from signals on mass 28 ($^{28}N_2$). In the second setup, $Na^{15}NO_3^-$ (98 atom% ^{15}N, Isotec) was added to the overlying water to a final $^{15}NO_3^-$ concentration of 40 to 50 µmol l^{-1}, resulting in varying relative ^{15}N-NO_3^- enrichment. Denitrification rates calculated from this setup are potential rates excluding NO_3^- limitation. During incubation, the signals for the masses of O_2, $^{28}N_2$, $^{29}N_2$ ($^{14}N^{15}N$) and $^{30}N_2$ ($^{15}N^{15}N$) were monitored.

Isotope pairing technique/sub-core incubations. In September 2009, sub-cores were sampled and used for isotope pairing. To apply the IPT (Nielsen 1992, Steingruber et al. 2001), $^{15}NO_3^-$ concentrations in the overlying water were adjusted to 0, 25, 50, 100 and 150 µmol l^{-1} with 3 replicates for each concentration. Cores were capped with gas-tight plungers fitted with stirring devices, and incubated at *in situ* temperature for up to 24 h. After incubation, we homogenized the entire sediment of each core and preserved 3 sample batches of the resulting slurry with 100 µl of a 50% (wt/vol) $ZnCl_2$ solution in 15 ml glass vials. Vials were stored at 4°C and analysed within 2 wk.

Laboratory analyses and rate determinations

Nutrient concentrations and nutrient fluxes. Nutrient concentrations were determined photometrically with an automated continuous flow system (Bran & Luebbe Auto Analyzer 3) using standard methods of seawater analysis (Grasshoff et al. 1999). The relative error of triplicate sample measurements was below 1.5% for nitrate, nitrite and phosphate concentrations, and below 5% for ammonium concentrations. Nutrient fluxes during flow through incubations were calculated according to Eq. (1) (see 'Flux calculations' below).

Sediment characteristics. At each site, we determined sediment characteristics of one sediment core cut into 1 cm slices of known volume down to 10 cm. These slices were frozen for transport and stored until analysis in the laboratory.

Water content and porosity were calculated assuming a grain density of 2.65 g cm^{-3}. Grain size distribution was determined by sieving dry samples through mesh sizes of 1000 µm, 500 µm, 250 µm, 125 µm and 63 µm. The weight percentages of total nitrogen (TN) and organic carbon (C_{org}) were determined with an Elemental Analyser (Thermo Flash EA) calibrated against acetanilide. The standard deviation of duplicate analyses was below 0.05% for C_{org} and below 0.005% for TN.

Determination of N_2 and O_2 concentrations with MIMS. The concentrations of N_2 (mass 28, 29 and 30 in case of amended cores) and O_2 in water overlying incubated sediments were calculated from N_2/Ar and O_2/Ar ratios determined with a MIMS system consisting of a quadrupole mass spectrometer (QMS) (GAM 200, InProcess Instruments) with a modified membrane inlet (Bay Instruments). The QMS ion source produces O^+ ions by ionizing sample gas which can react with N_2 forming NO^+ (Eyre et al. 2002). This so-called NO^+-effect may result in higher signals on mass 28 at low oxygen concentrations and low mass 28 signals at high oxygen concentrations, and thus may lead to a misinterpretation of N_2 generated by denitrification. The NO^+-effect was tested for the MIMS system used here, and was found to be below the standard deviation of the method (0.1%) (J. Pohlmann pers. comm.). Concentrations of $^{29}N_2$ and $^{30}N_2$ were calculated based on the excess signals of mass 29 and 30, as described in detail in An et al. (2001).

Air-saturated temperature-salinity-standards prepared according to Kana et al. (1994) were used to correct instrumental offsets in N_2/Ar and O_2/Ar ratios. Concentrations of N_2 and O_2 were calculated by multiplying the corrected N_2/Ar and O_2/Ar ratios with the Ar concentration (as a function of temperature and salinity) from solubility tables (Weiss 1970).

Flux calculations. Sediment N_2 and O_2 fluxes of continuous flow incubations were calculated as follows:

$$fl = (C_o - C_i) \times f / a \quad (1)$$

where C_i and C_o are inflow and outflow concentations, respectively, f is the flow rate (l h^{-1}) and a is sediment surface (m^2). Net N_2 and O_2 fluxes of the unamended cores were calculated from signals on masses 28 and 32, respectively, whereas the N_2 generated in ^{15}N-amended cores was monitored for $^{28}N_2$, $^{29}N_2$ and $^{30}N_2$ simultaneously.

Calculation of denitrification rates from sub-core incubations according to IPT. Denitrification rates in sub-core incubations with added $^{15}NO_3^-$ and ambient $^{14}NO_3^-$ were calculated according to equations used in the classical IPT (Nielsen 1992, Steingruber et al. 2001). IPT assumes that the N_2 species ($^{28}N_2$, $^{29}N_2$ and $^{30}N_2$) produced after $^{15}NO_3^-$ addition are generated in ideal binominal proportions, so that denitrification of ambient $^{14}NO_3^-$ can be derived from the production rates $p^{29}N_2$ and $p^{30}N_2$. These were calculated from the N_2 concentrations, $c(N_2)$, measured by MIMS on masses 29 and 30 as follows:

$$p(N_2) = [c(N_2) / (a \cdot t)] \cdot (V_w + V_s \cdot \varphi) \quad (2)$$

where p is the production rate, c is N_2 concentration, a is the sediment surface area (m^2), t is the incubation time (h), V_w is the overlying water volume, V_s is the sediment volume, and φ is the porosity.

From N_2 production rates, denitrification rates of $^{15}NO_3^-$ (D_{15}: µmol N m^{-2} h^{-1}) were derived as:

$$D_{15} = 2 \times (p^{30}N_2) + (p^{29}N_2) \quad (3)$$

Denitrification rates of ambient $^{14}NO_3^-$ (D_{14}: µmol N m^{-2} h^{-1}) were calculated as:

$$D_{14} = [(p^{29}N_2) / 2 \times (p^{30}N_2)] \times D_{15} \quad (4)$$

The total denitrification rate (D_{tot}) is the sum of D_{14} and D_{15}.

To estimate the proportion of coupled nitrification-denitrification (D_n) as opposed to denitrification of nitrate only from the overlying water (D_w), we applied:

$$D_w [\%] = (D_{15}/\varepsilon) \times 100 / D_{tot} \quad (5)$$

where ε represents the relative $^{15}NO_3^-$ enrichment over natural abundance during the incubation.

From Eqs. (4) and (5), we estimate coupled nitrification-denitrification D_n as

$$D_n [\%] = 100 - D_W \quad (6)$$

RESULTS

Site characteristics

Bottom water nutrient concentrations at sampling sites were higher in March than in September, accompanied by low water temperatures of around 6°C compared to 15–19°C in September (Table 1). Dissolved nutrient concentrations of bottom waters were highest in the inner Elbe Estuary (Stns ML to KL) and decreased rapidly towards coastal stations (Stns TR, TS and further northwards). March nitrate

concentrations ranged from 263 µmol l^{-1} at Stn ML to 58 µmol l^{-1} at Stn WW. In September, nitrate concentration in the inner estuary (Stns ML to KL) was between 30 and 100 µmol l^{-1}, and decreased to 2–8 µmol l^{-1} towards the inner coastal stations (Stns TR, TS), dropping below the detection limit at stations further northwards (Stns BOS to HT).

Sampling sites were selected so that sediment properties varied between stations and reflected dominant sediment types and ranges of organic carbon concentrations (Table 1). Relatively fine-grained sediments (median grain size of around 63 µm) with high porosity (up to 0.9) were sampled within the inner Elbe Estuary. These sediments also had the highest organic carbon and nitrogen concentrations (3.4 % and 0.4 %, respectively). More coarse-grained sediment types (median grain size of 125 µm and porosities around 0.4) dominated at sites outside the estuary. From Stn BOS northwards, sediments were mostly sandy with low to undetectable organic carbon and nitrogen concentrations (Table 1).

Nutrient fluxes

In the sediment incubations, we measured mean net nitrate and ammonium fluxes (averages of 3 to 6 cores) across the sediment-water interface. Nitrate fluxes were directed into the sediment (negative signs denoting flux into the sediment) in both seasons, whereas ammonium flux directions varied (Fig. 2). Increased influxes after $^{15}NO_3^-$ addition occurred at most stations in March and September.

Nitrate fluxes into sediments tended to decrease with distance from the inner Elbe Estuary. Highest nitrate influxes (up to −187 ± 46 µmol m^{-2} h^{-1} at Stn ML; Fig. 1) were observed at stations within the upper Elbe Estuary and did not differ significantly between March and September campaigns. In contrast, nitrate fluxes further downstream (Stns NW, KL and TS) were lower in September than in March.

Ammonium fluxes were directed into the sediment in March, with highest fluxes at stations in the upper estuary, decreasing with distance from the port of Hamburg. In contrast, sediments were a source of ammonium in September. We found maximum effluxes of 343 ± 10 and 224 ± 24 µmol m^{-2} h^{-1} at Stns ML and KL, respectively. At all other stations, ammonium fluxes were much lower (~10 µmol m^{-2} h^{-1}). Ammonium fluxes did not change significantly with $^{15}NO_3^-$ addition in either of the sampling campaigns.

Table 1. Site and sediment characteristics for the sampling stations. Porosity, organic carbon content and nitrogen content are given as average values for 10 sediment slices from one core of 10 cm length (slice resolution: 1 cm); median grain size is given for the entire 10 cm; bdl = below detection limit; nd = not determined

	Station	T (°C)	Salinity	Water depth (m)	pH	PO_4^- (µmol l^{-1})	NH_4^+ (µmol l^{-1})	NO_3^- (µmol l^{-1})	Porosity (v/v)	N (%)	C_{org} (%)	Median grain size (µm)	Oxygen penetration depth (mm)
March 2009	ML	6.7	0.3	2.9	8.3	2.9	8.7	263	0.8	0.2	2.4	<63	2.9
	STS	6.6	0.4	4.6	8.2	2.6	5.7	278	0.7	0.1	0.7	63	>35
	BR	4.8	0.5	1.9	8.4	2.6	3.7	284	0.6	0.1	1.5	63	3.2
	NW	6.3	0.6	3.3	8.2	3	3.3	285	0.5	0.0	0.3	63	3.7
	KL	6.5	10	1.9	8.3	3.6	4	194	0.5	0.1	0.6	63	3.6
	TS	5.8	22	2.8	8.4	2.9	4.9	89	0.4	bdl	0.1	125	6.5
	WW	5.8	23	5.3	8.4	2	5.8	58	0.4	bdl	0.1	125	4.2
September 2009	ML	18.2	0.4	1.4	7.5	1.2	8.4	86.8	0.9	0.4	3.4	<63	1.9
	STS	18.9	0.8	1	7.8	2.8	0.4	99.9	0.3	bdl	0.0	250	4.2
	BR	18.1	5.2	0.7	7.9	4.4	1.2	96.6	0.4	bdl	0.1	63	3.6
	NW	18	8	3.7	8	4.5	1.5	88.1	0.7	0.1	1.4	63	1.3
	KL	16.7	23	3.8	8.2	3	2.1	30.1	0.5	bdl	0.3	63	2.9
	TR	16.1	28	7.9	8.2	2	4	7.9	0.5	bdl	0.2	125	3.5
	TS	16.3	29	5.7	8.3	1.3	2	2.2	0.5	bdl	0.1	63	2.1
	BOS	16.1	29	3.9	8.3	1.2	1.7	bdl	0.4	bdl	0.2	125	2.3
	FP	16	30	3.5	8.3	0.7	1.2	bdl	0.4	bdl	bdl	125	3.2
	SOS	15.7	30	4.1	8.2	0.7	1.3	bdl	0.4	bdl	bdl	125	nd
	KO	15.9	31	3.9	8.3	0.4	1.2	bdl	0.4	bdl	bdl	125	2.4
	HT	16.1	31	3.8	8.3	0.6	1.1	bdl	0.4	bdl	bdl	125	nd

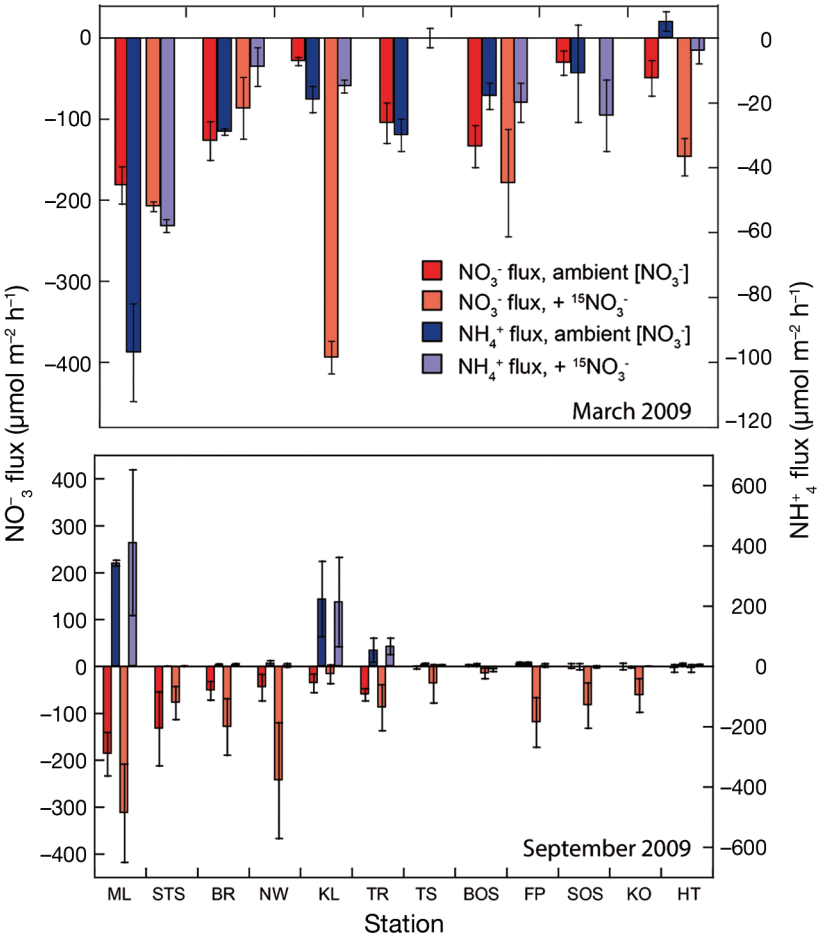

Fig. 2. Ammonium and nitrate fluxes during continuous flow incubation of amended (+$^{15}NO_3^-$) and unamended sediment cores for the sampling campaigns in March and September 2009

N_2 and O_2 fluxes during continuous flow incubation

The oxygen uptake of sediments (sediment oxygen demand, SOD; see 'Laboratory analyses and rate determinations' above) in the whole-core incubations was generally higher in September than in March. During the September campaign, SOD was highest (–1360 µmol m^{-2} h^{-1}) in the upper estuary (Stns ML and STS), and decreased rapidly within the estuary following the general spatial pattern of N_2 release. At distal stations in the Wadden Sea (Stns FP to HT; Fig. 1), N_2 fluxes dropped below 8 µmol N m^{-2} h^{-1}, accompanied by a decrease in SOD to values of 170 to 390 µmol m^{-2} h^{-1} (data not shown). A similar decrease in overall O_2 fluxes with distance to the estuary was observed in March, but the flux of O_2 into the sediment was roughly half the September rate in the inner estuary (Fig. 3B), and decreased at coastal stations to a flux comparable to that of September.

We did not detect water column denitrification in any of the control incubations; denitrification was solely due to sedimentary processes. Generally, stations with a high SOD showed high N_2 effluxes, with small seasonal variations in the upper Elbe Estuary. N_2 fluxes consequently showed the same general pattern of high fluxes in the upper estuary and decreasing fluxes at offshore stations. Within the estuary up to Stn NW, N_2 fluxes were generally higher in September than in March. An exception was Stn TS outside the estuary, where $^{28}N_2$ fluxes in March were higher than in September (Fig. 3) and corresponded to higher ambient nitrate concentration in March (Table 1). This dependence on nitrate concentration was shown in a strong decrease of $^{28}N_2$ fluxes at all stations north of Stn TR, and also shows in the increased N_2 production upon $^{15}NO_3^-$ addition to the core incubations (α = 0.05). This adds evidence to our assumption that N_2 fluxes were often limited by nitrate concentration.

Denitrification rates from sub-core incubation and IPT

In addition to continuous flow incubations of intact sediment, we also applied a combined sub-core incubation and IPT at 7 stations in September 2009. These 2 data sets provide independent control of calculated denitrification rates, and can also shed light on pathways of N_2 conversion, as discussed below.

To compare denitrification rates derived from the combined IPT/sub-core incubation assay with the denitrification rates obtained by continuous flow incubation (Fig. 4), we assumed that 1 µmol N_2 flux m^{-2} h^{-1} is equal to 2 µmol of denitrified NO_3^- m^{-2} h^{-1}. We found that the difference between both rate estimates was within the standard deviations of average denitrification rates at all sites except Stn KL, where the IPT-derived rate was slightly higher than the rate determined with the continuous flow incubation technique. Thus, both methods yield comparable results under the given conditions (Fig. 4). Furthermore, we found no dependence of $^{29}N_2$ production on the amount of added label in all but one of the stations sampled in September 2009 (data not shown).

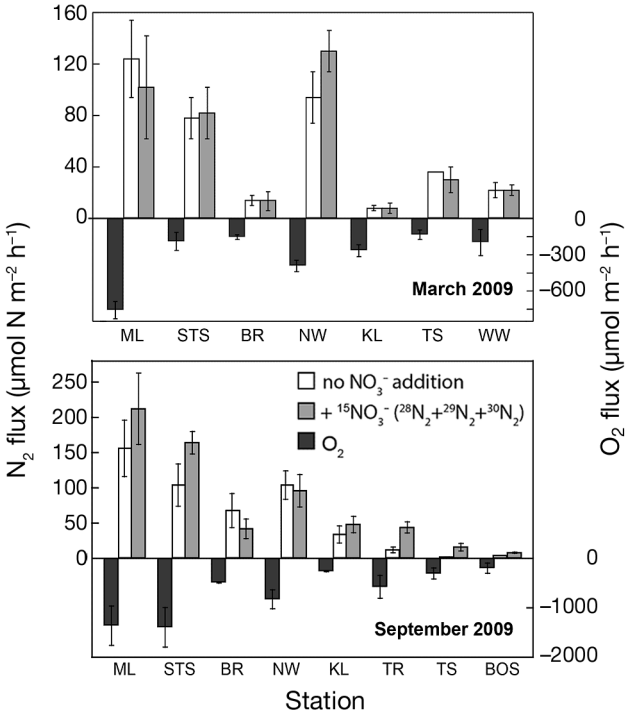

Fig. 3. N_2 and O_2 fluxes in intact sediment cores. Data are shown separately for incubations at ambient nitrate concentrations and upon $^{15}NO_3^-$ addition in March and September 2009. Stations with N_2 fluxes of less than 4 µmol m^{-2} h^{-1} are not shown for sake of clarity. Oxygen flux is based on mean values of both incubations

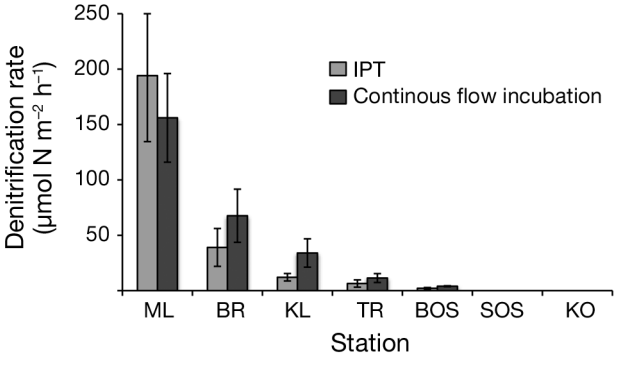

Fig. 4. Comparison of denitrification rates calculated according to sub-core incubation and isotope pairing technique (IPT), and rates derived from continuous flow incubation of intact sediment cores at ambient nitrate concentration

DISCUSSION

We evaluated N_2 fluxes as indicators of sediment N_r loss in shallow water zones of the Elbe Estuary and the adjacent coastal zone exposed to the nitrate load of the Elbe River plume. Our combination of sediment incubations at ambient nitrate concentration and incubations with added $^{15}NO_3^-$ allowed us to quantify net N_2 production rates, and to recognize individual N_2 production processes based on isotope pairing. This combined assay differentiates between different N_2 production pathways, allows estimates of their relative contribution, and also traces changed N_2 production triggered by label addition. In the first part of our discussion, we accordingly estimate the proportion of N-cycling pathways that contribute to the net N_2 flux. In the second part, we discuss factors affecting N_2 production, such as nitrate concentration, organic matter availability, and SOD. Finally, we roughly estimate annual nitrogen removal rates in the shallow water zones in the tidal Elbe Estuary, and their capacity to reduce the N_r load of the Elbe River plume.

Sources and sinks of N_2 in the estuary

In a comparison between denitrification rates as estimated from direct N_2 flux measurements of incubated cores and rates obtained by IPT/sub-core incubations, the 2 different methods yielded comparable results (Fig. 4). A further benefit of this comparison is that it permits estimates of coupled nitrification-denitrification and N_2 fixation at the 7 sites analysed with the 2 techniques in September 2009.

While the reasons for N_2 fixation in heterotrophic, N-rich environments are speculative, this process is increasingly gaining attention (Fulweiler et al. 2007, Bertics et al. 2010), and accordingly, we wanted to evaluate its role in sediments from the Elbe Estuary. The comparison of IPT and N_2/Ar fluxes offers an excellent means to investigate the importance of nitrogen fixation: when no N_2 fixation occurs, denitrification rates obtained from IPT should match denitrification rates calculated from $^{28}N_2$ fluxes (An et al. 2001), whereas denitrification rates derived from $^{28}N_2$ flux should be lower than those derived from IPT (see Eq. 4) if N_2 fixation was significant. Our data show similar rates from both techniques (Fig. 4) and imply that N_2 fixation is negligible in sediments of the Elbe Estuary and adjacent coastal zone. Consequently, the $^{28}N_2$ flux measured in the unamended cores is a good approximation of the gross N_2 production in the intact sediment cores.

Besides denitrification, anammox is a candidate pathway for N_r removal. It couples the reduction of nitrite (NO_2^-) to the oxidation of ammonium (NH_4^+), and also produces N_2 gas (Thamdrup & Dalsgaard 2002, Trimmer & Nicholls 2009). In the IPT experiments in September 2009, we used different $^{15}NO_3^-$

concentrations to evaluate the role of anammox. The underlying assumption of IPT is that the added $^{15}NO_3^-$ does not interfere with the denitrification rate of ambient $^{14}NO_3^-$ (Steingruber et al. 2001), and that the evolving N_2 species ($^{28}N_2$, $^{29}N_2$ and $^{30}N_2$) in this case follow an ideal binominal distribution. If, in contrast, anammox were a significant process, $^{15}NO_3^-$ addition should promote $^{29}N_2$ production stemming from $^{15}NO_2$ (deriving from $^{15}NO_3^-$ reduction) and oxidation of $^{14}NH_4^+$ (Risgaard-Petersen et al. 2003). D_{14} calculated according to Eqs. (2) to (4) would in this case include an unknown offset caused by the increased $^{29}N_2$ production during anammox. Accordingly, a correlation of the calculated D_{14} with $^{15}NO_3^-$ concentration suggests that the calculated rates are influenced by a certain portion of N_2 production from anammox.

In our study area, however, we found that anammox was apparently of little importance. Regardless of $^{15}NO_3^-$ concentration, the calculated D_{14} did not vary in all but one station, suggesting little or no contribution from anammox to N_2 fluxes from sediments of the Elbe Estuary in September 2009. The only exception was Stn BR, where D_{14} increased linearly with increasing $^{15}NO_3^-$ addition (data not shown). We thus conclude that anammox may have contributed to the relatively high overall N_2 production of 68 ± 24 µmol N m^{-2} h^{-1} at this particular station. Overall, the limited importance of anammox is in accordance with our expectations that N-loss in heterotrophic shallow regions is affected by denitrification (Thamdrup & Dalsgaard 2002, Thamdrup 2012).

N_2 production in our experiments did not always keep pace with nitrate uptake into the sediments. DNRA, the dissimilative reduction of nitrate to ammonium, is a candidate nitrate sink and could also explain ammonium effluxes from the sediment. However, our nitrate addition experiments suggest that it may not be a dominant process in the Elbe Estuary: DNRA is stimulated by the addition of nitrate (Gardner et al. 2006, Koop-Jakobsen & Giblin 2010), and this should lead to increased ammonium release rates in amended versus unamended cores. This clearly was not the case in our experiments, as ammonium release rates were comparable in both experimental setups (Fig. 2). Moreover, ammonium release is more pronounced at high organic matter concentrations, as a comparison between March and September data clearly shows (Fig. 2, Table 1). Thus, we assume that remineralisation is a more important contributor to ammonium release than DNRA, although we note that the evaluation of net fluxes, as in our experiment, cannot quantitatively resolve all internal processes (Lin et al. 2011).

A potential alternative sink for nitrate in our system besides denitrification is uptake by either benthic microalgae — which can be considerable even in the dark — or by the heterotrophic bacterial community, especially in turbid estuaries (Middelburg & Nieuwenhuize 2000a,b). Such uptake can bind dissolved nitrate in organic matter. Thus, an important distinction in terms of actual N_r loss from the system is the differentiation between denitrification of nitrate from the overlying water (direct denitrification), and denitrification of nitrate generated from remineralized organic matter by nitrification (coupled nitrification-denitrification or indirect denitrification), which is often particularly important in nutrient-rich coastal systems (Laursen & Seitzinger 2002). We calculated the contribution of coupled nitrification-denitrification to total N_2 production in September 2009 via IPT. This assay is based on $^{29}N_2$ and $^{30}N_2$ production from $^{15}NO_3^-$ amended cores (Nielsen 1992, Steingruber et al. 2001). The relative contribution of coupled nitrification/denitrification was 36% at Stn ML, 32% at Stn KL, 43% at Stn TR, and 97% at Stn BOS. Overall, the estimates of direct versus indirect denitrification in September thus suggest that denitrification of water column nitrate prevailed in sediments of the Elbe Estuary (Stns ML to KL). With decreasing nitrate concentration further downstream, indirect denitrification gained in relative importance and dominated bulk denitrification (at relatively low rates) at Stn BOS.

We did not register nitrate efflux from the sediment at any station; thus, sediment nitrification did not produce more nitrate than was being internally turned over. However, the sediment ammonium uptake in September was much less pronounced than in March. At 3 stations (Stns ML, KL and TR), sediments actually changed from being a net sink for ammonium in March to being a net source of ammonium to the water column. This may be due to increased remineralisation of organic matter, which is appreciably higher in September than in March at the 2 stations with highest ammonium release (Table 1, Fig. 2). The high ammonium fluxes also highlight the potential importance of nitrification — reoxidizing up to 30% of ammonium in the oxic sediment layer (Sweerts et al. 1991) — both in sediments and presumably also the water column of the estuary.

Influences on denitrification rates of sediments in the Elbe Estuary

Low temperatures suppress most microbial processes (e.g. Koch et al. 1992), and we accordingly

expected higher N_2 production in September (water temperatures 16 to 18°C) than in March (around 6°C; Table 1). However, we found that the effect of temperature was limited: while N_2/Ar measurements revealed an overall increase in N_2 production rates in September compared to March 2009 (Fig. 3), the intensity of this increase was highly variable, with N_2 production rates in March occasionally even exceeding the rates in September (Fig. 3). Clearly, there are additional controls of N_2 production, and likely candidates are the sediment C_{org} content and nitrate concentration in the overlying water column (Seitzinger & Nixon 1985, Seitzinger 1988, Van Luijn et al. 1999, Deutsch et al. 2010).

A statistical analysis of relationships between gas fluxes, sediment properties, and nutrient concentration for March and September indeed reveals that denitrification rates are correlated to C_{org} concentration, ambient [NO_3^-] and only to a much lesser degree, temperature. The highest N_2 fluxes (34 to 156 µmol N m^{-2} h^{-1}) were observed in sediments within the Elbe Estuary (Stns ML to NW) that are exposed to highest nitrate concentrations and have medium to high C_{org} content (Table 1).

That nitrate is indeed a major controlling factor for N_2 production in the sediments is also borne out by differences between N_2 fluxes in cores with and without $^{15}NO_3^-$ addition in September 2009 (Fig. 3). At Stn KL and further northwards, where the ambient nitrate concentration was low (Table 1), N_2 fluxes were significantly higher in incubations with added nitrate, suggesting that the bottleneck for denitrification in this area is bottom water nitrate. This means that coastal sediments remove significant amounts of N_r only as long as NO_3^- substrate is available; whereas this denitrification ceases when the river nitrate load is low during the summer months. In the summer, the sediments further away from the river plume do not receive significant amounts of nitrate, as water column nitrate concentration is already depleted due to phytoplankton assimilation (see also Sørensen et al. 1979, Pätsch et al. 2010, Deek et al. 2011).

A further control of denitrification rates is organic matter availability in the sediment. Addition of $^{15}NO_3^-$ concentrations of 40 to 50 µmol l^{-1} to cores from the nitrate-limited coastal sampling sites (Stns KL to HT) in September 2009 did not result in N_2 fluxes by any means comparable to that of stations close to the river mouth (Fig. 3). These sediments have low C_{org} concentrations (<0.2%, Table 1), whereas the active sediments within the estuary are exposed to high perennial nitrate concentrations and have high organic carbon contents: here, conditions are ideal for denitrification, which proceeds at high rates in our incubations regardless of the season.

Estimate of N_2 fluxes based on SOD

The limited effect of temperature on denitrification rates was unexpected. We suspect that this is due to superposition of effects that depend on temperature, but also have a strong impact on water column nitrate concentration or organic matter load; an example for such a process is primary production. Accordingly, an integrated measure of biological productivity may offer further insights into denitrification dynamics, and we thus analysed a possible correlation of denitrification and SOD.

In an extensive review of denitrification studies, Seitzinger & Giblin (1996) found a strong positive correlation of N_2 fluxes and SOD in continental shelf sediments. In both March and September 2009, we found a similar positive correlation of N_2 fluxes and SOD (Fig. 5). The slope derived from our data (0.101) was similar to, but lower than the slope which has been reported for denitrification in estuarine and freshwater systems (0.142; cf. Seitzinger & Giblin 1996 and references therein). Intriguingly, it aligns well with the slope the authors found for continental shelf systems (0.116; Seitzinger & Giblin 1996), in which denitrification is mainly fed by coupled nitrification/denitrification, and not by water column nitrate. In our setting, however, our calculations of indirect denitrification suggest that denitrification is fuelled by water column nitrate at the majority of stations. These rates of direct denitrification differ regionally as a function of bottom water nitrate concentrations and organic matter availability (Seitzinger & Giblin 1996, Deutsch et al. 2010, Deek et al. 2011), as seen in the gradient of relative contributions of direct versus indirect denitrification in our data set as described above. Nevertheless, and regardless of seasonal differences and spatial heterogeneities, our comparison shows that SOD offers a solid basis to estimate denitrification rates. Errors in this estimate may arise from ignoring regional or even local factors that regulate N_2 production, which suggests that such regional factors need to be taken into account wherever possible.

Estimate of denitrification in the estuary

In historical times, denitrification was pronounced in the inner Elbe Estuary (Dähnke et al. 2008 and ref-

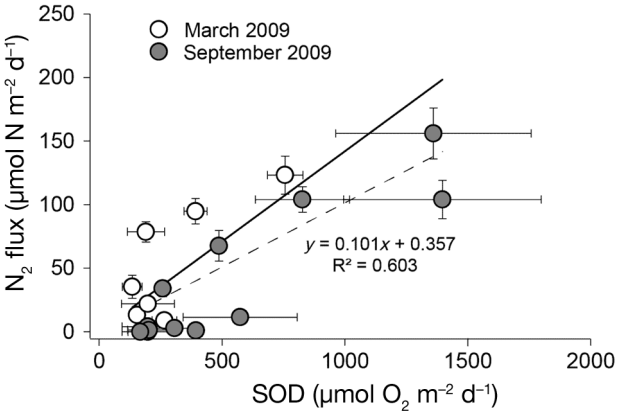

Fig. 5. N_2 fluxes in March and September versus sediment oxygen demand (SOD). Solid line indicates theoretical denitrification rates (µmol N as N_2 m^{-2} h^{-1}) calculated according to Seitzinger & Giblin (1996)

erences therein), with a pronounced nitrate removal along the estuarine salinity gradient. This decrease was not visible in later times; but despite this, Schröder et al. (1996) used sediment incubations to investigate nitrogen cycling, and found high sediment denitrification rates in the upper estuary. Since these investigations, dredging and deepening of the riverbed has continued. Construction activities such as diking and deepening led to an increase in the tidal range of the Elbe Estuary (from 2.6 m in 1963 to 3.6 m in 2004), a dramatic reduction in shallow water and intertidal areas, and to higher current velocities (ARGE 2004, Heise et al. 2005). Moreover, backwaters of the Elbe such as the Mühlenberger Loch (our Stn ML) were partially or even completely removed. Deepening the ship channel has also removed fine-grained sediment types and underlying sandy layers from the river bed, and exposed compacted glacial moraines (Kerner & Jacobi 2005).

These processes can alter sediment composition and their capability for denitrification. Nitrogen loss rates decrease with increasing channel depth (Alexander et al. 2000), and these changes in river structure limit the ability of sediments in the estuary to act as an efficient nutrient filter for sites further downstream. Accordingly, we wanted to use our estimates of denitrification to gauge changes in the overall denitrification capacity of the estuary. Our statistical analysis revealed that denitrification in the estuary depends mainly on nitrate concentration and total organic carbon (TOC), with, surprisingly, a minor influence of temperature. Our study sites covered a range of different sediment types and were spread over the entire estuary. To extrapolate our rates, we used literature data on the spatial extent of sediment types around our study sites and their mean TOC content (Miehlich et al. 1997, Gröngröft et al. 2006). The resulting correlation is robust (r^2 = 0.55; Fig. 6) and comparable to that of N_2 production to SOD (Fig. 5). Based on the relationship between [TOC], [NO_3^-], temperature and resulting N_2 production, we extrapolated denitrification rates to the entire estuary from the Port of Hamburg to the transition to the German Bight (Stn KL).

We obtained N_2 production rates of 15.4 and 15.5 t N d^{-1} in March and September, respectively. Over the course of spring and summer months (March to September), we calculated an average total N_2 production of 3.3 ± 1.2 kt N in the estuary. Interestingly, and supporting this approach, an extrapolation based on SOD (see Fig. 5) yields a similar estimate that falls within the uncertainty of our calculation (2.6 ± 0.2 kt N).

Comparing our estimate to nutrient loads for this time of year (47 kt), averaged for the years 2001 to 2009 (J. Pätsch pers. comm.), ~7% of the total annual nitrate load is converted to N_2 during the spring and summer months on transit through the estuary. We did not sample within the ship channel, so our estimate does not include denitrification possibly occurring in artificially exposed coarse-grained and compacted sediment types (glacial sands and tills) exposed by dredging. Nevertheless, it represents a maximum estimate, as denitrification capacity is known to decrease with channel depth (Alexander et al. 2000), while our estimate includes deep sediments

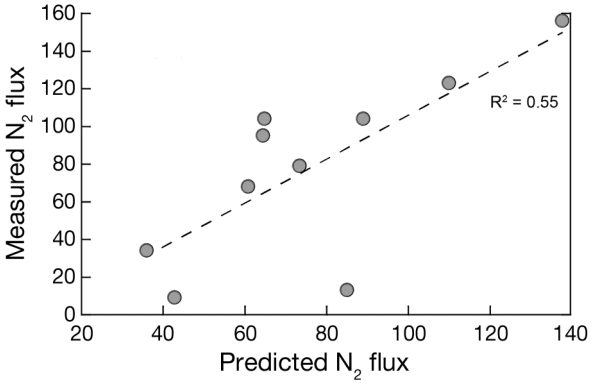

Fig. 6. Comparison of measured and predicted N_2 production (µmol N m^{-2} h^{-1}) in the inner Elbe Estuary. The predicted N_2 production is based on empirical relationships between measured [NO_3^-], sediment [TOC] and temperature (T). The multivariate regression equation for predicted N_2 production is $-35.2 + 0.16[NO_3^-] + 12.06[TOC] + 2.68\,T$, represented by the dashed line. Grey circles show N_2 production in continuous flow incubations in the inner estuary (Stns ML to KL, and the corresponding prediction

that are exposed to rapid water flow, which limits sediment-water interaction and nutrient transformation and retention (Haggard et al. 2001).

This calculation of present-day denitrification (7% of fluvial N_r) implies a drastic decrease compared to the 40% summertime nitrate removal Schröder et al. (1996) calculated for the Elbe Estuary in the early 1990s. That denitrification in today's sediments of the Elbe Estuary is near negligible is in accordance with a study by Dähnke et al. (2008) who found that nitrate behaves mostly conservatively in the brackish section of the estuary. Judging from differences in nitrate relationships to salinity, they estimated a maximum nitrate loss of 5 to 10% in summertime. Our data support this and allow a more precise quantification of this change in estuarine filter function. Obviously, sediments in the modern, managed Elbe Estuary are far from effectively attenuating riverine nitrate inputs.

There could be many reasons for this gradual decrease: on-going construction has changed the sediment and hydromorphology to conditions that are much less favourable for denitrification, and one of the main controlling factors — nitrate concentration — has decreased (Radach & Pätsch 2007, Pätsch & Lenhart 2011). However, this nitrate decrease has not kept pace with diminishing denitrification capacity, so that current nitrate loads are discharged almost undiminished into the outer estuary. In the adjacent Wadden Sea, intertidal and sub-tidal sediments partly counteract these massive nitrate discharges (Deek et al. 2011, Gao et al. 2012).

CONCLUSIONS

Human activity has markedly increased the N_r inputs into the Elbe River and adjacent coastal zone of the German Bight. After years of declining loads, we expect rising concentrations of nitrate resulting from increased biofuel production in the river catchment. The sediments in the estuary can be very effective nitrate sinks: high nitrate concentrations in water in contact with organic-carbon-rich sediments in the estuary cause high denitrification rates that could, in principle, attenuate significant amounts of river-borne nitrate. However, the capacity of sediments in the Elbe Estuary to eliminate nitrate by denitrification has suffered from dredging and removal of backwater areas. While remaining sediments continue to actively remove nitrate in the inner Elbe Estuary, their overall capacity is much reduced due to shrinking areas of submersed natural sediments compared to historical levels — removing no more than 3.3 ± 1.2 kt N during spring and summer months, or 7% of the total nitrate load of the Elbe River. The remainder is channelled to the coastal North Sea, where intertidal sediments only partly eliminate nitrate in the overlying water delivered by the Elbe River plume. We observed that sediment denitrification in summer months is limited by nitrate availability at the fringe of the river influence, whereas non-limiting nitrate supply reveals a second limitation by organic matter content in sandy sediments. The highest denitrification rates were found in the inner estuary, where the high N_2 production rate does not vary significantly with temperature and nitrate concentrations. This suggests that the riparian zones operate at maximum denitrification efficiency, and that a further reduction of their spatial coverage would further diminish denitrification capacity of the estuary.

Acknowledgements. We thank the Helmholtz Zentrum Geesthacht, Institute for Coastal Research and the DFG (Em 37/29) for financial support. The IfBM of University of Hamburg and the FTZ Westküste (Büsum) are acknowledged for providing laboratory space. We thank W. S. Gardner and M. J. McCarthy (Marine Science Institute, University of Texas at Austin) for their gracious introduction to sediment incubation work. Captain H. Bornhöft and the crew of the RV 'Ludwig Prandtl' are acknowledged for help and assistance during our sampling campaigns, and N. Lahajnar and F. Langenberg (IfBM, University of Hamburg) helped with the data set of sediment characteristics.

LITERATURE CITED

Alexander RB, Smith RA, Schwarz GE (2000) Effect of stream channel size on the delivery of nitrogen to the Gulf of Mexico. Nature 403:758–761

An S, Gardner WS, Kana TM (2001) Simultaneous measurement of denitrification and nitrogen fixation using isotope airing with membrane inlet mass spectrometry. Appl Environ Microbiol 67:1171–1178

ARGE (2004) Sauerstoffhaushalt der Tideelbe. Arbeitsgemeinschaft für die Reinhaltung der Elbe. Available at www.fgg-elbe.de/dokumente/fachberichte.html

Bertics VJ, Sohm JA, Treude T, Chow CET, Capone DG, Fuhrman JA, Ziebis W (2010) Burrowing deeper into benthic nitrogen cycling: the impact of bioturbation on nitrogen fixation coupled to sulfate reduction. Mar Ecol Prog Ser 409:1–15

Brockmann UH, Kattner G (1997) Winter-to-summer changes of nutrients, dissolved and particulate organic material in the North Sea. Dtsch Hydrogr Z 49:229–242

Conley DJ, Kaas H, Mohlenberg F, Rasmussen B, Windolf J (2000) Characteristics of Danish estuaries. Estuaries 23: 820–837

Dähnke K, Bahlmann E, Emeis K (2008) A nitrate sink in estuaries? An assessment by means of stable nitrate isotopes in the Elbe estuary. Limnol Oceanogr 53:1504–1511

Day J, Kemp CAS, Kemp WM, Yanez-Arancibia A (eds) (1989) Estuarine ecology. John Wiley & Sons, New York, NY

Deek A, Emeis K, van Beusekom J (2011) Nitrogen removal in coastal sediments of the German Wadden Sea. Biogeochemistry 108:467–483

Deutsch B, Forster S, Wilhelm M, Dippner J, Voss M (2010) Denitrification in sediments as a major nitrogen sink in the Baltic Sea: an extrapolation using sediment characteristics. Biogeosciences 7:3259–3271

Erisman JW, Sutton MA (2008) Reduced nitrogen in ecology and the environment: special issue of the ESF-FWF conference in partnership with LFUI, October 2006. Environ Pollut 154:357–358

Eyre BD, Rysgaard S, Dalsgard T, Christensen PB (2002) Comparison of isotope pairing and N_2:Ar methods for measuring sediment denitrification — assumptions, modifications, and implications. Estuaries 25:1077–1087

Fulweiler RW, Nixon SW, Buckley BA, Granger SL (2007) Reversal of the net dinitrogen gas flux in coastal marine sediments. Nature 448:180–182

Gao H, Matyka M, Liu B, Khalili A and others (2012) Intensive and extensive nitrogen loss from intertidal permeable sediments of the Wadden Sea. Limnol Oceanogr 57: 185–198

Gardner WS, McCarthy MJ, An S, Sobolev D, Sell KS, Brock D (2006) Nitrogen fixation and dissimilatory nitrate reduction to ammonium (DNRA) support nitrogen dynamics in Texas estuaries. Limnol Oceanogr 51:558–568

Gardner WS, Seitzinger SP, Malczyk JM (1991) The effects of sea salts on the forms of nitrogen released from estuarine and freshwater sediments: Does ion pairing affect ammonium flux? Estuaries 14:157–166

Grasshoff K, Ehrhardt M, Kremling K (eds) (1999) Methods of seawater analysis, 3rd edn. Wiley-VCH, Weinheim

Gröngröft A, Grabowski K, Schwank S (2006) Umweltverträglichkeitsuntersuchung 'Anpassung der Fahrrinne der Unter- und Außenelbe an die Containerschiffahrt'. Teilgutachten zum Schutzgut Wasser, Teilbereich Sedimente. Unpublished report, Institute of Soil Science, University of Hamburg

Haggard BE, Storm DE, Tejral RD, Popova YA, Keyworth VG, Stanley EH (2001) Stream nutrient retention in three northeastern Oklahoma agricultural catchments. Trans ASAE 44:597–605

Heise S, Calmano W, Ahlf W, Leal W, Krahn D (2005) Environmental challenges for the Hamburg stretch of the River Elbe and its catchment with regard to the Water Framework Directive. www.watersketch.net/WP4_Dissemination_of_results/Handbook/vdo_ws_05_study_germany_elbe.pdf (accessed 17 Aug 2010)

Kana TM, Darkangelo C, Hunt MD, Oldham JB (1994) Membrane inlet mass spectrometer for rapid high-precision determination of N_2, O_2, and Ar in environmental water samples. Anal Chem 66:4166–4170

Kerner M, Jacobi A (2005) Die Elbevertiefung von 1999. Tatsächliche und prognostizierte Auswirkungen. WWF Deutschland, Frankfurt am Main

Koch MS, Maltby E, Oliver GA, Bakker SA (1992) Factors controlling denitrification rates of tidal mudflats and fringing salt marshes in south-west England. Estuar Coast Shelf Sci 34:471–485

Koop-Jakobsen K, Giblin AE (2010) The effect of increased nitrate loading on nitrate reduction via denitrification and DNRA in salt marsh sediments. Limnol Oceanogr 55: 789–802

Laursen AE, Seitzinger SP (2002) The role of denitrification in nitrogen removal and carbon mineralization in Mid-Atlantic Bight sediments. Cont Shelf Res 22:1397–1416

Lavrentyev PJ, Gardner WS, Yang L (2000) Effects of the zebra mussel on nitrogen dynamics and the microbial community at the sediment-water interface. Aquat Microb Ecol 21:187–194

Lin X, McCarthy MJ, Carini SA, Gardner WS (2011) Net, actual, and potential sediment–water interface NH_4^+ fluxes in the northern Gulf of Mexico (NGOMEX): evidence for NH_4^+ limitation of microbial dynamics. Cont Shelf Res 31:120–128

Lozán JL, Kausch H (1996) Warnsignale aus Flüssen und Ästuaren. Parey, Berlin

McCarthy MJ, Gardner WS (2003) An application of membrane inlet mass spectrometry to measure denitrification in a recirculating mariculture system. Aquaculture 218: 341–355

Middelburg JJ, Nieuwenhuize J (2000a) Nitrogen uptake by heterotrophic bacteria and phytoplankton in the nitrate-rich Thames estuary. Mar Ecol Prog Ser 203:13–21

Middelburg JJ, Nieuwenhuize J (2000b) Uptake of dissolved inorganic nitrogen in turbid, tidal estuaries. Mar Ecol Prog Ser 192:79–88

Middelburg JJ, Soetaert K, Herman PMJ, Heip CHR (1996) Denitrification in marine sediments: a model study. Global Biogeochem Cycles 10:661–673

Miehlich G, Gröngröft A, Jähnig U, Neuschmidt O, Walter F, Franke S, Schwartz R (1997) Umweltverträglichkeitsstudie 'Anpassung der Fahrrinne der Unter- und Außenelbe an die Containerschiffahrt'. Materialband III: Fachgutachten Sedimente, Hamburg

Nielsen LP (1992) Denitrification in sediment determined from nitrogen isotope pairing. FEMS Microbiol Ecol 86: 357–362

Nielsen LP, Brotas V, Viaroli P, Underwood GJC and others (2000) Protocol handbook for NICE: nitrogen cycling in estuaries. A project under EU research programme: marine science and technology (MAST III). National Environmental Research Institute, Silkeborg

Nixon SW, Ammerman JW, Atkinson LP, Berounsky VM and others (1996) The fate of nitrogen and phosphorus at the land sea margin of the North Atlantic Ocean. Biogeochemistry 35:141–180

Pätsch J, Lenhart H-J (2011) Daily nutrient loads of nutrients, total alkalinity, dissolved inorganic carbon and dissolved organic carbon of the European continental rivers for the years 1977–2009. Berichte aus dem Zentrum fuer Meeres- und Klimaforschung, Reihe B: Ozeanographie. Zentrum für Meeres- und Klimaforschung, Hamburg

Pätsch J, Serna A, Dähnke K, Schlarbaum T, Johannsen A, Emeis KC (2010) Nitrogen cycling in the German Bight (SE North Sea) — Clues from modelling stable nitrogen isotopes. Cont Shelf Res 30:203–213

Radach G, Pätsch J (2007) Variability of continental riverine freshwater and nutrient inputs into the North Sea for the years 1977–2000 and its consequences for the assessment of eutrophication. Estuaries Coasts 30:66–81

Risgaard-Petersen N, Nielsen LP, Rysgaard S, Dalsgaard T, Meyer RL (2003) Application of the isotope pairing technique in sediments where anammox and denitrification coexist. Limnol Oceanogr Methods 1:63–73

Schröder F, Wiltshire KH, Klages D, Mathieu B, Knauth HD (1996) Nitrogen and oxygen processes in sediments of

the Elbe estuary. Arch Hydrobiol 110(Suppl 110):311–328

Seitzinger SP (1988) Denitrification in freshwater and coastal marine ecosystems: ecological and geochemical significance. Limnol Oceanogr 33:702–724

Seitzinger SP, Giblin AE (1996) Estimating denitrification in North Atlantic continental shelf sediments. Biogeochemistry 35:235–274

Seitzinger SP, Nixon SW (1985) Eutrophication and the rate of denitrification and N_2O production in coastal marine sediments. Limnol Oceanogr 30:1332–1339

Sørensen J, Jørgensen BB, Revsbech NP (1979) Comparison of oxygen, nitrate, and sulfate respiration in coastal marine sediments. Microb Ecol 5:105–115

Steingruber SM, Friedrich J, Gächter R, Wehrli B (2001) Measurement of denitrification in sediments with the ^{15}N isotope pairing technique. Appl Environ Microbiol 67: 3771–3778

Sweerts J, Bargilissen MJ, Cornelese AA, Cappenberg TE (1991) Oxygen-consuming processs at the profundal and littoral sediment water interface of a small meso-eutrophic lake (Lake Vechten, The Netherlands). Limnol Oceanogr 36:1124–1133

Thamdrup B (2012) New pathways and processes in the global nitrogen cycle. Annu Rev Ecol Evol Syst 43: 407–428

Thamdrup B, Dalsgaard T (2002) Production of N_2 through anaerobic ammonium oxidation coupled to nitrate reduction in marine sediments. Appl Environ Microbiol 68: 1312–1318

Trimmer M, Nicholls JC (2009) Production of nitrogen gas via anammox and denitrification in intact sediment cores along a continental shelf to slope transect in the North Atlantic. Limnol Oceanogr 54:577–589

van Beusekom JEE, Weigelt-Krenz S, Martens P (2008) Long-term variability of winter nitrate concentrations in the Northern Wadden Sea driven by freshwater discharge, decreasing riverine loads and denitritication. Helgol Mar Res 62:49–57

Van Luijn F, Boers PCM, Lijklema L, Sweerts J (1999) Nitrogen fluxes and processes in sandy and muddy sediments from a shallow eutrophic lake. Water Res 33:33–42

Weiss RF (1970) The solubility of nitrogen, oxygen and argon in water and seawater. Deep-Sea Res Oceanogr Abstr 17:721–735

Editorial responsibility: William Kemp, Cambridge, Maryland, USA

Submitted: December 17, 2012; Accepted: August 13, 2013
Proofs received from author(s): October 28, 2013